

## AN EXPERIMENTAL STUDY ON ULTIMATE STRENGTH OF COMPOSITE COLUMNS FOR COMPRESSION OR BENDING

*By Hiroshi NAKAI\*, Osamu YOSHIKAWA\*\* and Hiromasa TERADA\*\*\**

This paper reports the test results of composite columns subjected to compression or bending in order to investigate the properties of ultimate strength of concrete filled rectangular steel columns with thin-walled steel plates.

In the compression tests of composite columns, the effects of headed studs and longitudinal stiffeners on the behaviors in elasto-plastic regions are examined experimentally in comparisons with the concrete filled columns without headed studs and longitudinal stiffeners. Their ultimate strengths are, then, discussed on the basis of theoretical analysis. On the other hand, the influences of end diaphragms and studs, which restrain the slips between encased concrete and steel tubular plates, upon the composite effects and the corresponding ultimate strength for flexural behaviors are also examined by means of the bending tests.

*Keyword : composite structures, bridge piers, tests, ultimate strength.*

### 1. INTRODUCTION

The reinforced concrete structures have mainly been adopted to the piers of highway bridges because of their economical points of view. However, the cross-sectional dimensions of such type of structures become generally larger and much more reinforcements are required for resisting the strong seismic load. Therefore, it seems that the ordinary reinforced concrete piers are not always suitable ones.

In the case of steel pier composed of comparatively small cross-sectional dimensions, thick steel plates and many longitudinal stiffeners will be needed to ensure the safety against the overall and local bucklings under seismic loading. Thus, these types of piers are not economical ones.

In order to eliminate these demerits, a concrete filled steel pier (thereafter referred to as composite column), which utilizes the high tensile strength of steel tubular plates and the enough compressive strength of encased concrete, is considered to be of an appropriate type. Then, various researches on the composite columns have been executed in not only Japan but also foreign countries.

Among them, there have already been codified the design specifications for applying to the bridge structures such as BS 5 400<sup>1)</sup> and DIN 18 806<sup>2)</sup>. These kinds of researches are currently starting in Japan to applying the composite columns to the bridge piers of highways and mono-railway, i. e., one finds a series of experimental studies on the concrete-filled steel pipes by Public Work Research Institute of Japan Ministry of Construction<sup>3)</sup> and on the composite columns with the rectangular cross-sections by Hanshin Expressway Public Corporation<sup>4)</sup>. In applying these composite columns to the bridge piers, it is an

\* Member of JSCE, Dr. Eng., Professor, Dept. of Civ. Eng., Osaka City Univ. (Sugimoto 3-3-138, Sumiyoshi, Osaka 558)

\*\* Member of JSCE, Chief Engineer, First Construction Dept. of Osaka, Hanshin Expressway Public Corporation (Kita-kagaya 2-11-8, Suminoe, Osaka 559)

\*\*\* Member of JSCE, Chief Researcher, Research Institute, Yokogawa Bridge Works Ltd. (Shinminato 88, Chiba 260)

important problem how to design the steel tubular plates against the local buckling for the case of rectangular cross-section, since the ultimate strength of such composite columns will be somewhat different from the composite columns with circular cross-section. With regard to these researches, one can find a theoretical study reported by Reference 5). The validity of this theory is, however, not yet checked by the experimental researches. Accordingly, a series of tests were performed on the composite columns with rectangular cross-section under the conditions of compression or bending to inquire the validities of analysis in Reference 5) and especially the variations of ultimate strength due to the following uncertain factors which will not be able to analyze theoretically.

These factors are summarized follows;

- i) Effects of restrictions of encased concrete on the ultimate strength of steel tublar plates,
- ii) Influences of headed studs and longitudinal stiffeners on the behaviors in elasto-plastic region of composite columns and on the ultimate strength,
- iii) Effects of restrictions against the slips between encased concrete and steel tubular plates by means of end diaphragms and shear connectors on the composite behaviors in bending, as well as,
- iv) the occurrence of local buckling in compression flange of composite columns which undergo the bending.

This paper predicates such uncertain points in details.

2. TEST SPECIMENS

Table 1 shows the objects of experimental studies explained in the above together with loading conditions, length, symbols and numbers of test specimens. Their cross-sectional dimensions, buckling parameter, cross-sectional area and material properties are listed in Table 2.

The thickness of steel plates is limited within 4.2 mm to simulate the initial imperfections of ordinary structures by using mild steel made of Grade SS 41.

The length of specimens,  $a=800$  mm, for compression tests is decided so as to prevent the overall buckling of columns and to cause the local bucking of steel tubular plates.

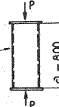
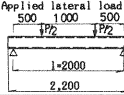
The cross-sectional dimensions of specimens for bending tests are identical to those of column specimens of no stiffener. The corresponding spans,  $l=2\ 000$  mm, are decided to be within the length of the space of our testing machine and the local buckling in the compression side of steel sections predominates rather than the overall lateral buckling as a beam.

The residual stresses in the test specimens are measured by the modeled test specimens, which have the same dimensions as Specimens, SC-1, SCL-1 and SCL-2, through the mechanical cutting method prior to the failure tests. These results can be modified as shown in Fig.1.

3. COMPRESSION TESTS

(1) Aims of tests

Table 1 Outline of Tests.

Test category	Loading condition length of column or span of beam	Symbol of test specimen (number)	Purpose of test
Compression test	Applied axial load 	SC-1, SC-2, SC-3, (3) CC-1, CC-2, CC-3, (3) CCS-1, CCS-2, CCS-3, (3) SCL-1, SCL-2, (2) CCL-1, CCL-2, (2)	The effect of i) encased concrete ii) shear studs (S) iii) longitudinal stiffeners (L) on ultimate strength of composite column
Bending test	Applied lateral load 	SB-1, SB-2, (2) CB-1, CB-2, (2) CBE-1, CBE-2, (2) CBS-1, CBS-2, (2)	The effects of i) end diaphragms (E) ii) shear studs (S) on ultimate strength for composite beam

Remarks ; SC : Steel Column, CC : Composite Column, SB : Steel Beam, CB : Composite Beam

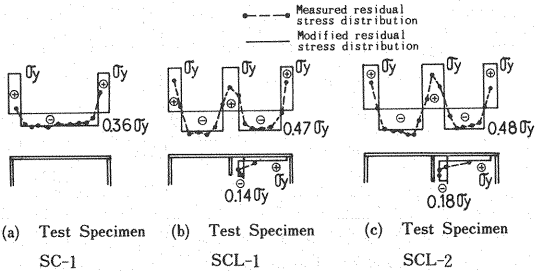
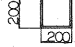
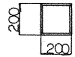
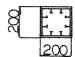


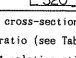
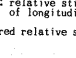


Fig.1 Residual Stress Distribution in Test Specimens.

Table 2 Cross-Sectional Dimensions and Material Properties.

Symbol of test specimen, (Number)	Cross-section of column or beam (mm)	Dimension of shear studs and longitudinal stiffeners	Cross sectional area		Properties of steel (MPa)		Properties of concrete (MPa)	
			steel tube $A_s$ (cm <sup>2</sup> )	concrete $A_c$ (cm <sup>2</sup> )	Yield point $\sigma_s$	Young's mod. $E_s$	Strength $\sigma_{ck}$	Young's mod. $E_c$
SC-1, SC-2, SC-3 SB-1, SB-2, (5)		n=1 b=192 t=4.2 b/t=45.7	32.9	—	320	$2.20 \times 10^5$	—	—
CC-1, CC-2, CC-3 CB-1, CB-2, (5) CBE-1, CBE-2, (7)		n=1 b=192 t=4.2 b/t=45.7	32.9	367.1	320	$2.20 \times 10^5$	22.6	$2.67 \times 10^4$
CCS-1, CCS-2, CCS-3 CBS-1, CBS-2, (5)		n=1 b=192 t=4.2 b/t=45.7 Shear studs 72-M4×30mm	32.9	367.1	320	$2.20 \times 10^5$	22.6	$2.67 \times 10^4$
SCL-1		n=2 b=254 t=3.0 b/t=42.3 4-Longitudinal stiffeners 3.0 × 42 mm * $\delta = 0.162$ , $\alpha = 0.98$ ** $\gamma_{1/7, req} = 0.837$	35.9	—	354	$2.23 \times 10^5$	—	
CCL-1			35.9	640.2			22.6	$2.67 \times 10^4$
SCL-2		n=2 b=314 t=3.0 b/t=52.3 4-Longitudinal stiffeners 3.0 × 51 mm * $\delta = 0.159$ , $\alpha = 2.50$ ** $\gamma_{1/7, req} = 1.07$	44.2	—	354	$2.23 \times 10^5$	—	
CCL-2			44.2	979.8			22.6	$2.67 \times 10^4$

\*  $\delta = nA_s/bt$ ;  $A_s$ : cross-sectional area of longitudinal stiffener $\alpha = a/b$ : aspect ratio (see Table 1)\*\*  $\gamma = I_1/I_2/(bt^3)$ : relative stiffness;  $I_1$ : geometrical moment of inertia of longitudinal stiffener $\gamma_{1/7, req}$ : required relative stiffness according to JSMB<sup>(3)</sup>

In the case of concrete filled column without headed studs, their steel tubular plates have the tendency to separate from the encased concrete for a case where the axial compressive force falls within the elastic ranges, since the Poisson's ratio of concrete,  $\mu_c \approx 1/6$ , is smaller than that of steel,  $\mu = 0.3$ . As the applied axial compressive force increases, the encased concrete will result in the plastic state. For this state, the Poisson's ratio of encased concrete increases up to  $\mu_c = 0.5$  and is greater than that of steel. Thus, the steel tubular plates undergo the internal pressure due to the transverse expansion of encased concrete.

This internal pressure will generally be resisted by the hooping force of the steel tubular plate in a case of circular cross-section. It is, then, clarified that the encased concrete reduces to the tri-axial compressive situations and their plastic flow is prevented by the hooping force of steel tubular plates.

Accordingly, the encased concrete cooperates with the steel tube as a composite column. This will, moreover, be able to strengthen the composite column with circular cross-section against the local buckling of steel tubular plates and the squashing of encased concrete.

In the case of composite column with rectangular cross-section, there remains an uncertain point concerning the hooping actions as compared with a composite column with circular cross-section and the behaviors of steel tubular plates under the internal pressure of encased concrete in the plastic state. In connection with this behavior, the effects of headed studs and longitudinal stiffeners on the ultimate strength of composite column have not also been clarified experimentally.

In order to investigate these problems, the compression tests were carried out.

## (2) Test method

The uniform and uniaxial compressive force was applied to the test specimens by avoiding the eccentricity through the thick loading pads at both the ends of columns. The applied loads were returned two- or three-times to 49 kN at a point where the gradient of load-axial shortening curve of test specimens had some change, and the residual deformations of test specimens

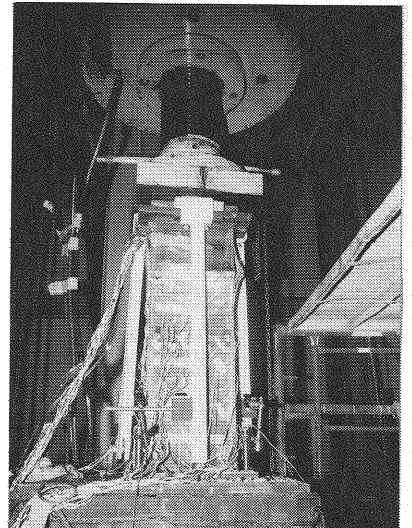


Photo 1 View of Compression Test.

were measured and checked. Thereafter, the applied load was gradually increased up to the failure of test specimens. The test view using a hydraulic jack with capacity of 5.88 MN, which is installed as the Bridge and Structural Laboratory of Osaka City University, is shown in Photo 1.

The measurements of strain at the typical points and shortening throughout the composite column were conducted by the strain gages and a displacement transducer in each loading stage, respectively.

### (3) Test results and their discussions

a) Effects of encased concrete on ultimate strength of column and buckling modes of steel tubular plates

Fig. 2 shows the load-strain curves at the sides of column (a), (b), (c) and (d) of Specimens SC-1 and CC-1. Observing this figure, the local buckling is propagated in the steel column SC-1 at the applied load  $P=490\sim 588$  kN and this column collapses with the slight increase of load after local buckling of steel tubular plates.

Whereas, the axial compressive strains gradually increase in the composite column Specimen CC-1 and the local buckling of steel tubular plates is not observed as in a case of steel column Specimen SC-1. The gradient of load-strain curve is altered at the load  $P\cong 930$  kN. This might be caused by the change to the plastic state of encased concrete. The Poisson's ratio of concrete, then, becomes large in accordance with the increase of load, and the steel tubular plates undergo not only compressive force but also lateral force due to the expansion of concrete. Thus, the local buckling of steel tubular plates towards the inside of encased concrete is completely prevented and the considerable increase of strength can be obtained by the superposed strength behaviors of steel tubular plates and encased concrete.

The local buckling modes of steel tubular plates after the collapse of each test specimen are plotted in Fig. 3.

It seems from the local buckling modes of steel columns, shown in Fig. 3 (a), (d) and (f), that the steel plates are bowed alternatively in the forms of convex and concave surfaces with the nodes at the corners of columns and longitudinal stiffeners and these steel tubular plates can, therefore, be treated as a compressive plate with the simply supported at the corners of column and longitudinal stiffeners.

On the other hand, the buckling modes of composite columns are in a pattern where all the steel plates bow out-sides of composite columns as shown in Fig. 3 (b), (c), (e) and (g) together with Photo 2.

This means that the steel tubular plates in composite columns can be dealt with one having all the edges clamped at the corners of columns and longitudinal stiffeners.

b) Effects of headed studs on restrictions of buckling of steel tubular plates

The headed studs in Specimens CCS-1~3 do not contribute to resisting the shearing force between steel plates and encased concrete but have a contribution to prevent the local buckling of steel plates

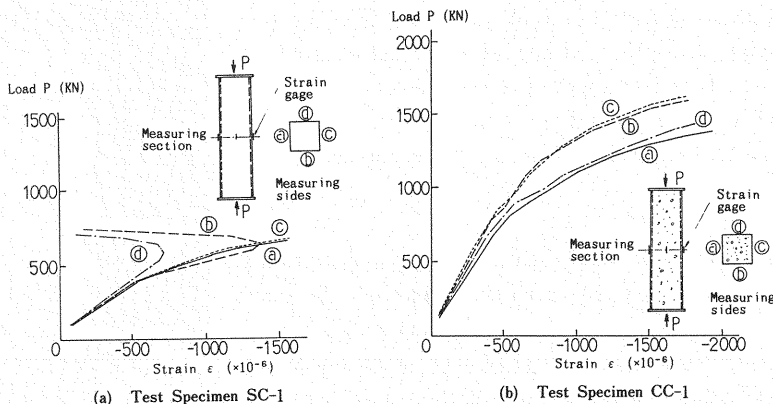


Fig. 2 Relationship between Load and Strain for Column.

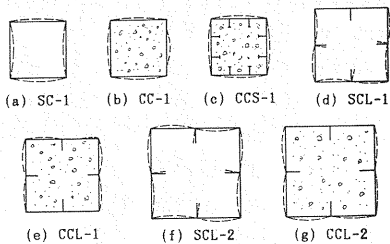


Fig. 3 Buckling Modes of Column Test Specimens.

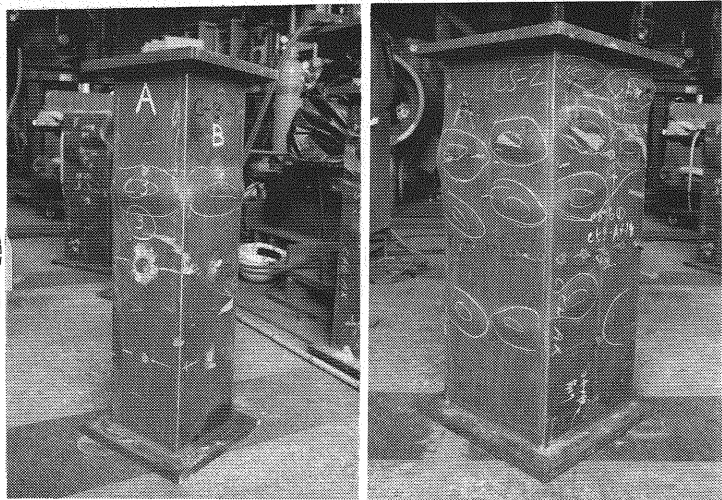


Photo 2 Buckling Modes of Composite Column.

towards the out-side of composite columns.

Fig. 4 shows the relationships between applied load and induced axial strain and force of headed studs in Specimens CC 1~3.

It is clear from this figure that the headed studs of the three Specimens CCS-1~3 undergo the tensile forces even in the lower loading stages and two Specimens CCS-2, 3 have a tendency to increase the tensile force of headed studs suddenly when the applied load exceeds approximately 1 200 kN in CCS-2 and 1 700 kN in CCS-3. These large tensile forces of headed studs may be caused by the restrictions against the local buckling of steel tubular plates.

Then, the local buckling of steel tubular plates is more or less prevented by the pull-out resistant forces due to the anchoring effect and frictions between headed studs and encased concrete, which is greater than ordinary bond forces, because the encased concrete is in high compressive stress situation. However, the remarkable effects of the headed studs on prevention of local buckling of steel tubular plates due to headed studs can not be expected, because the encased concrete is considered to be in the plastic state and is not effective for preventing the local buckling of steel tubular plates in these loading stages.

c) Effects of friction between longitudinal stiffener and encased concrete on restriction of local

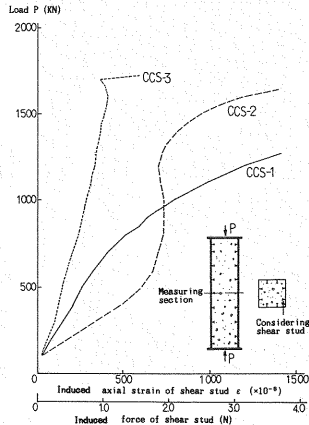


Fig. 4 Relationship between Load and Strain of Tensile Force of Headed Stud.

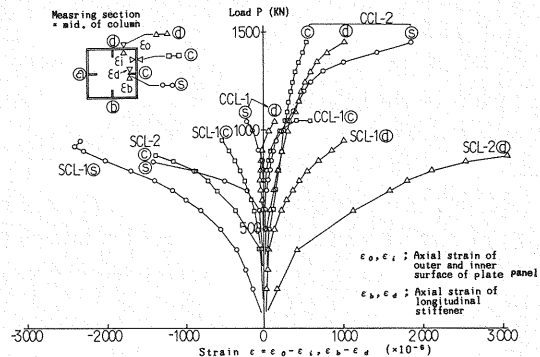


Fig. 5 Relationship between Load and Strain for Column with Longitudinal Stiffeners.

### buckling of steel tubular plates

For the longitudinal stiffeners in composite columns, the restrictions against the local buckling of steel tubular plates due to the bond and/or frictional forces of encased concrete will be expected together with the ordinary stiffening effects. Furthermore, the cross-sectional dimensions and the flexural rigidities of longitudinal stiffeners can be decreased because the local buckling of longitudinal stiffeners is prevented by the encased concrete.

Fig. 5 shows a load-axial strain curves at the center of plate panels and a measuring point 10 mm apart from the edge of longitudinal stiffeners in mid-section of Specimens SCL-1, 2 and CCL-1, 2.

It can be seen from Figs. 5 and 3 (d) that the buckling of stiffened plate takes place in the case of steel column SCL-1. While, Fig. 5 and Photo 2 (b) indicate that all the steel tubular plates of CCL-1 and CCL-2 bow with the buckling modes towards the out-side of composite columns.

This may be caused by the increase of flexural and torsional rigidities of longitudinal stiffeners encased with concrete and the prevention of buckling towards the inside of composite columns, thereby the steel tubular plates buckle locally under the boundary conditions with all the edges clamped.

The post-buckling strength is, of course, larger than that of steel column. It was observed by stripping the steel tubular plates from the composite columns after failure tests that the encased concrete was squashed and granulated at the point where the longitudinal stiffeners were deformed due to the local buckling of steel tubular plates, thus a considerable amount of restraint could not be expected by the encased concrete.

#### d) Ultimate load for compression

The ultimate load,  $P_c^*$  (average  $P_c$ ) of each test column is listed in Table 3, where the calculated values are obtained by a superposed method of ultimate load of steel tubular plates and encased concrete as follows;

$$\text{buckling load : } P_b = \sigma_b \cdot A_s + \beta \sigma_{ck} \cdot A_c \quad (1 \cdot a)$$

$$\text{squash load : } P_s = \sigma_y \cdot A_s + \sigma_{ck} \cdot A_c \quad (1 \cdot b)$$

in which,  $\sigma_b$  can be approximated by the local buckling strength of steel tubular plates without or with longitudinal stiffeners according to Literature 5) and Table 2, i. e.,

##### i) For steel column;

$$\sigma_b / \sigma_y = 1.0 \quad (R_s \leq 0.5) \quad (2 \cdot a)$$

$$= 0.390(R_s - 0.5)^2 - 0.911(R_s - 0.5) + 1.0 \quad (0.5 < R_s \leq 1.0) \quad (2 \cdot b)$$

$$= -0.146R_s + 0.015/(R_s - 0.8) + 0.713 \quad (R_s > 1.0) \quad (2 \cdot c)$$

##### ii) For composite column;

$$\sigma_b / \sigma_y = 1.0 \quad (R_f \leq 0.5) \quad (3 \cdot a)$$

$$= 0.433(R_f - 0.5)^2 - 0.831(R_f - 0.5) + 1.0 \quad (0.5 < R_f \leq 1.3) \quad (3 \cdot b)$$

where

$$R_s = 0.526 \cdot b / n t \cdot \sqrt{\sigma_y / E_s} \quad (4 \cdot a)$$

$$R_f = 0.323 \cdot b / n t \cdot \sqrt{\sigma_y / E_s} \quad (4 \cdot b)$$

$b$  : width of steel tubular plate,  $t$  : thickness of steel plate,  $n$  : number of plate panel,  $\sigma_y$  : yield point of steel,  $E_s$  : Young's modulus of steel

and

$\sigma_{ck}$  : nominal strength of encased concrete,  $A_s$  : cross-sectional area of steel tube,  $A_c$  : cross-sectional area of encased concrete,  $\beta$  : empirical reduction factor for strength of concrete  $\sigma_{ck}$  in buckling state of steel tubular plates, which can be presented as follows according to the test results;

$\beta = 0$  : for steel column

$$\beta \approx 0.7 : \text{for composite column } [=(P_b - \sigma_b A_s) / \sigma_{ck} A_c] \quad (5)$$

Table 4 shows the calculated results of  $R_s$ ,  $R_f$  and corresponding ratio  $\sigma_b / \sigma_y$ .

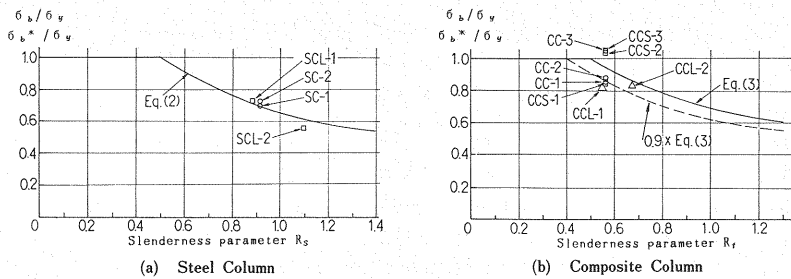
Observing Table 3, the test results,  $P_c^*$ , or  $P_c$ , are nearly equal to the local buckling load  $P_b$  and the

**Table 3** Comparisons of Test Results with Calculated Ultimate Load for Compression.

Test specimen	Test result of ultimate load (kN)		Calculated result (kN)		Ratio	
	$P_c^*$	Average $P_c$	Buckling load $P_b$	Squash load $P_s$	$P_c^*/P_b$ or $P_c^*/P_s$	$P_c^*/P_s$ or $P_c^*/P_s$
SC-1	735	748	723	1 052	1.03	0.71
SC-2	760					
CC-1	1 485	1 561	1 707	1 886	0.91	0.83
CC-2	1 509					
CC-3	1 691	1 607	1 707	1 886	0.94	0.85
CCS-1	1 467					
CCS-2	1 666	1 691	1 707	1 886	0.94	0.85
CCS-3	1 691					
SCL-1	926	—	898	1 270	1.03	0.73
CCL-1	2 058	—	2 463	2 725	0.84	0.76
SCL-2	872	—	945	1 564	0.92	0.56
CCL-2	2 871	—	3 254	3 792	0.88	0.76

**Table 4** Slenderness Parameter  $R_b$ ,  $R_f$  and Corresponding Strength  $\sigma_b/\sigma_y$ ,  $\sigma_b^*/\sigma_y$ .

Test specimen	Slenderness parameter		Buckling strength ratio	
	Steel column $R_f$	Composite column $R_b$	Analytical result $\sigma_b/\sigma_y$	Test result $\sigma_b^*/\sigma_y$
SC-1	0.917	—	0.688	0.699
SC-2				0.722
CC-1	—	0.563	0.949	0.857
CC-2				0.880
CC-3	—	0.563	0.949	1.053
CCS-1				0.840
CCS-2	—	0.563	0.949	1.029
CCS-3				1.053
SCL-1	0.885	—	0.707	0.729
CCL-1	—	0.544	0.964	0.818
SCL-2	1.095	—	0.604	0.558
CCL-2	—	0.672	0.870	0.839

**Fig. 6** Comparisons of  $\sigma_b^*/\sigma_y$  with  $\sigma_b/\sigma_y$  due to Slenderness Parameter  $R_b$  and  $R_f$ .

local buckling strength governs the ultimate strength of column rather than the squash strength.

In order to evaluate the local buckling strength of steel tubular plates, their test strengths,  $\sigma_b^*/\sigma_y$ , are predicted by modifying the test results  $P_u^*$  as follows ;

$$\sigma_b^*/\sigma_y = (P_u^* - \beta \cdot \sigma_{ck} \cdot A_c) / (A_s \cdot \sigma_y) \quad (6)$$

where  $P_u^*$  : local buckling load in tests

These results are listed in Table 4 and are also plotted as shown in Fig. 6.

By comparing  $\sigma_b^*/\sigma_y$  and  $\sigma_b/\sigma_y$ , a tendency to coincide with each other is recognized in the case of steel columns. However, it should be required further discussions for the case of composite columns concerning the following points ; ① non-linear characteristic of encased concrete, ② applicability of superposed strength method of steel and concrete, ③ eccentricity of applied compressive force during tests, ④ boundary condition and weld size of steel tubular plates in composite column along their edges and ⑤ effect of internal pressure of encased concrete due to the plasticization.

#### 4. BENDING TEST

##### (1) Aims of test

When the bending moment acts on a composite column, it is expected that the perfect composite effects will be obtained by preventing the slipping between interior surface of tubular plates and encased concrete through the perfectly rigid end diaphragms, shear connectors with infinitesimal intervals and so on. However, it is impossible to build such a composite column, then the elastic deformations of these members will occur and affect the local and overall flexural behaviors of composite columns. In addition to the above, the local buckling of flange plates in the compression side will govern the ultimate strength of composite column for bending. In order to know such uncertain points, the bending tests were carried out on eight column specimens.

(2) Test method

Lateral loads were applied at the quarter points,  $1/4\ l$ , of test specimens with the length,  $l=200\text{ cm}$ , to have the regions where pure bending and bending moments accompanied with shearing force are predominant in composite columns (see Table 1). Photo. 3 shows a typical view of bending test. The loads were applied to the test specimens controlled by load-and strain-velocity of testing machine in elastic and elasto-plastic ranges, respectively. The strains and displacements in the test specimens were, then, measured by setting the strain-velocity of testing machine equal to zero.

(3) Test results and their discussions

a) Effects of composite action

To investigate the differences of composite effects between Specimen CBE-1 with end diaphragms and CBS-1 with shear connectors (headed studs), the strain distributions at mid-length of them are plotted as shown in Fig. 7. It is obvious from this figure that the stress distributes almost linealy on the basis of elementary beam theory in both the specimens and their neutral axis is located at  $e=8.03\text{ cm}$  from the upper flange, which is also neary equal to that of beam theory  $e=7.83\text{ cm}$  calculated by using  $E_s=2.20\times10^5\text{ MPa}$ ,  $E_c=2.68\times10^4\text{ MPa}$  and ignoring the tensile part of concrete.

The load-slip curves between steel tubular plates and encased concrete for Specimens CB-1 without shear connectors and CBS-1 with shear connectors can be investigated from Fig. 8.

It is apparent from this figure that the slip is effectively prevented by shear connectors in Specimen CBS-1 compared with Specimen CB-1 of natural bond.

Fig. 9 shows the load-strain curves for the composite columns at a section where shearing force is predominant. These curves show that there are no remarkable differences between CBS-1 (with shear

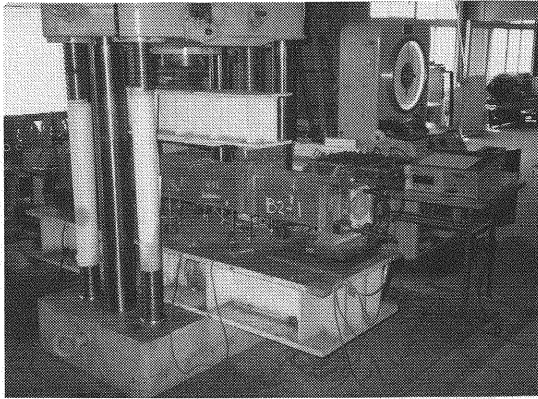


Photo 3 View of Bending Test.

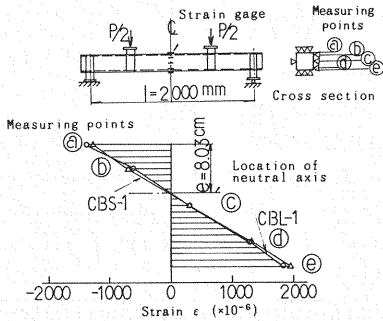


Fig. 7 Strain Distributions in Test Specimens CBL-1 and CBS-1 ( $P=245\text{ kN}$ )

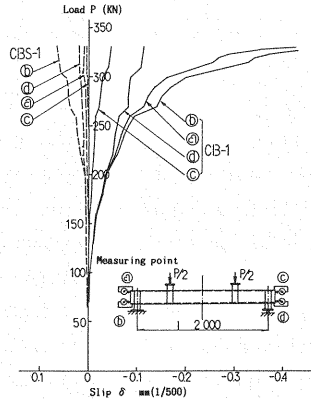


Fig. 8 Relationship between Load and Slip in Test Specimens CB-1 and CBS-1.

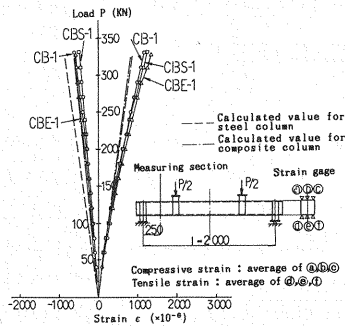


Fig. 9 Relationship between Load and Strain in Composite Columns.

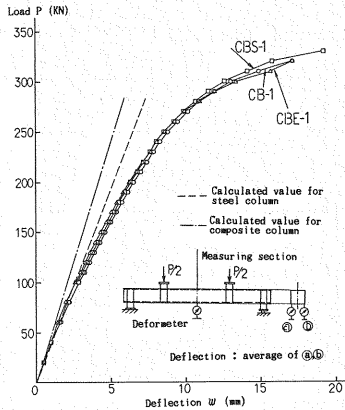


Fig. 10 Relationship between Load and Deflection in Composite Columns.

Table 5 Comparisons of Test Results with Calculated Ultimate Load for Bending.

Item Test specimen	Test results of ultimate load (kN) Original data $P_B^*$	Calculated load (kN)				Ratio		
		Average $P_B$	Elastic buckling load $P_{eB}$	Yield load $P_y$	Plastic load $P_p$	$P_e/P_B$	$P_y/P_B$	$P_p/P_B$
SB-1	255	248	162	269	309	1.53	0.92	0.80
SB-2	240							
CB-1	333	329	250	273	368	1.32	1.20	0.89
CB-2	324							
CBE-1	333	328	250	273	368	1.31	1.20	0.89
CBE-2	323							
CBS-1	343	333	250	273	368	1.33	1.22	0.90
CBS-2	323							

connectors), CBE-1 (with end diaphragms) and CB-1 (of natural bond).

Here it seems that the difference between test results and calculated ones results in the influence of out-of-plane deformation of compression flange plate near the loading points.

Finally, Fig. 10 shows the load-deflection curves at the mid-length of composite columns.

Likewise, a little difference of composite action between Specimens CBS-1, CBE-1 and CB-1 are observed from this figure. It is, however, concluded that the considerable composite effects can be obtained even in the case of natural bond such as Specimen CB-1.

#### b) Ultimate strength for bending

The test results,  $P_B^*$  (average  $P_B$ ) and the calculated ones corresponding to three ultimate states  $P_b$ ,  $P_y$  and  $P_p$  are summarized in Table 5, where

$$P_b = 8M_b / l \dots \dots \dots (7 \cdot a)$$

$$P_y = 8M_y / l \dots \dots \dots (7 \cdot b)$$

$$P_p = 8M_p / l \dots \dots \dots (7 \cdot c)$$

These loads correspond to local buckling moment  $M_b$ , yielding moment  $M_y$  of steel tubular plate, and fully plastic moment  $M_p$  of composite column, where the tensile part of encased concrete is ignored, respectively.  $M_b$ ,  $M_y$  and  $M_p$  can easily be estimated as follows;

$$i) \quad M_{cr} = M_b \text{ or } M_y$$

By referring to Fig. 11,  $M_{cr}$  leads to

$$M_{cr} = B/3 \{ \sigma_c \cdot (h_c + t)^2 + \sigma_t \cdot (h - h_c + t)^2 \} - b/3 \{ \sigma_c \cdot h_c^2 + \sigma_t \cdot (h - h_c)^2 \} + b/3 \cdot \sigma_c \cdot h_c^2 \dots \dots \dots (8 \cdot a)$$

where

$$h_c = n \cdot (B \cdot H - b \cdot h) / b + \sqrt{n \cdot (B \cdot H - b \cdot h) / b^2 + n(B \cdot H - b \cdot h) \cdot h / b}, \quad n = E_s / E_c \dots \dots \dots (8 \cdot b)$$

$$ii) \quad M_p$$

Similarly,  $M_p$  is gained from Fig. 12 as follows;

$$M_p = \sigma_y / 2 \cdot (2 \cdot h_c - h) \cdot [B \cdot (h + 2 \cdot t) - b \cdot h] + b/2 \cdot \sigma_{ck} \cdot h_c^2 \cdot \beta \dots \dots \dots (9 \cdot a)$$

where

$$h_c = n \cdot (B \cdot H - b \cdot h) / b + \sqrt{n \cdot (B \cdot H - b \cdot h) / b^2 + n(B \cdot H - b \cdot h) \cdot h / b}, \quad n = E_s / E_c \dots \dots \dots (9 \cdot b)$$

The failure of all the test specimens are caused by out-of-plane local buckling of steel plate near the loading points as sketched in Fig. 13.

In the steel columns SB-1, 2, the ultimate load  $P_b = 248$  kN seems to be significantly affected by this local buckling of steel plate and the steel columns fail prior to the yielding state. While, the composite columns have almost the same ultimate load,  $P_B = 328 \sim 333$  kN, and it seems that the local bucklings occur adjacent to the yielding state. However, it is pointed out that the composite columns with thin steel tubular

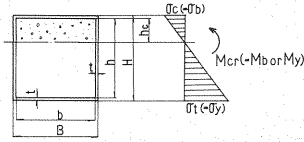


Fig. 11 Buckling or Yielding Moments  $M_b$ ,  $M_y$ .

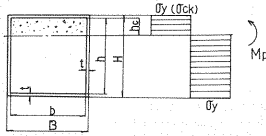


Fig. 12 Fully Plastic Moment  $M_p$ .

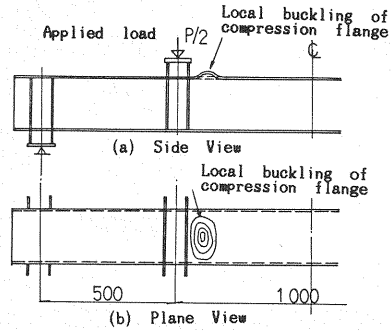


Fig. 13 Buckling Mode of Compression Flange of Composite Column.

plates do not reach the fully plastic state due to the local buckling of steel tubular plates.

In addition to these facts, the ultimate load of composite columns with only natural bond (SB-1 and SB-2) is not different from the other ones (CBE-1, 2 and CBS-1, 2). Therefore, the restrictions of slips between steel tubular plates and encased concrete may not be serious problems in designing the composite columns under bending.

## 5. Conclusion

This paper reports the experimental studies on the ultimate strength of composite columns made of thin-walled rectangular steel tubular plates and encased concrete.

The tests were carried out under the conditions of compression or bending by using the specimens with and without shear connectors (headed studs) and longitudinal stiffeners.

Firstly, the main conclusions obtained by compression tests are summarized as follows;

(1) The local buckling modes of steel tubular plates become nearly close to that of plate with a boundary condition where all the edges of plates are clamped. Then, the significant stiffening effects can be expected due to the encased concrete and a redundancy against the ultimate strength becomes large after the local buckling of steel plates.

(2) The local buckling of stiffened plate can also be prevented remarkably by the encased concrete, even when a case where the flexural rigidity of longitudinal stiffeners is small.

(3) Although the stiffening effects against the local buckling of steel plate due to the headed studs are not so much expected, but the post buckling strength is more or less increased.

(4) The test results of buckling strength of steel tube were well coincided with the calculated ones on the basis of Reference 5) in the case of steel column. For the buckling of steel tubular plate in composite column, the test results showed somewhat lower strength than the calculated ones in Reference 5), then it should require the further discussion to be applied to practical design.

Secondly, the results of bending tests can be concluded as follows;

(5) The ultimate bending strength of steel columns is governed by the local buckling strength of compression flanges. Whereas, that of composite column is not so affected by the local buckling of steel tubular plates and is determined by the yielding stress of steel plates.

(6) Thus, the encased concrete behaves to increase the ultimate strength of composite column. However, it is impossible to strengthen up to the fully plastic state because of the local buckling of steel tubular plates.

(7) A slight increase of flexural rigidity of composite columns due to end diaphragms and shear connectors, which prevent the slip between steel tubular plate and concrete, can be expected, but these effects are not noticeable.

(8) It is possible to build the composite column having enough strength and rigidity without using the closely arranged shear connectors or rigid end diaphragms.

### Acknowledgement

In conducting the experimental studies, the authors would like to acknowledge the valuable opinions given by Dr. M. Fujii, Associate Professor of Kobe University, and Dr. T. Kitada, Associate Professor of Osaka City University. The authors are also indebted to Mr. S. Kato, Mr. I. Nakamura and Mr. F. Hakamada, Hanshin Expressway Public Corporation as well as Mr. Y. Matsumoto and Mr. H. Mizoguchi, Research Institute of Yokogawa Bridge Works, Ltd., in excutions of tests.

### REFERENCES

- 1) British Standard Institution; BS 5400, Part 5, Code of practice of composite bridges, March 1980
- 2) DIN 18 806, Teil 1, Tragfähigkeit von Verbundstützen, Berechnung und Bemessung, Sept. 1981.
- 3) Public Work Research Institute of the Ministry of Construction; Load Bearing Force in Concrete-Filled Steel Pipes (No. 1), August 1981, Load Bearing Force in Concrete-Filled Steel Pipes (No. 2), May 1983, and Load Bearing Force in Concrete-Filled Steel Pipes (No. 3), May 1984.
- 4) Nakai, H. and Yoshikawa, O. ; Experimental Study on Strength of Concrete-Filled Steel Pier, Proc. of JSCE, No. 344, I-1, pp. 195~204, April 1984.
- 5) Nakai, H., Kitada, T. and Yoshikawa, O. ; A Design Method of Steel Plate Element in Concrete-Filled Square Steel Tubular Columns, Proc. of JSCS, No. 356, I-3, pp. 405~413, April 1985.
- 6) Japanese Road Association; Specifications for Highway Bridge (JSHB), Feb. 1980.

(Received October 14 1985)